Accurate and transferable extended Hückel-type tight-binding parameters

J. Cerdá* and F. Soria
Instituto de Ciencia de Materiales de Madrid, CSIC, Cantoblanco, 28049 Madrid, Spain
(Received 12 August 1999)

We show how the simple extended Hückel theory can be easily parametrized in order to yield accurate band structures for bulk materials, while the resulting optimized atomic orbital basis sets present good transferability properties. The number of parameters involved is exceedingly small, typically ten or eleven per structural phase. We apply the method to almost fifty elemental and compound bulk phases.

I. INTRODUCTION

Accurate electronic structure calculations that involve large unit cells still represent a major challenge in solid-state physics, primarily due to their high computer demands. Despite the recent development of highly efficient *ab initio*, density functional theory-based formalisms that scale linearly with the unit-cell size,[1] it is still a common procedure to study this type of systems with the use of (semi)-empirical tight-binding Hamiltonians that employ linear combinations of atomic orbitals (LCAO) as the basis. Following the Slater-Koster (SK) approach,[2] a preselected set of tight-binding parameters (TBP's) is fitted to accurate band structures that may either be calculated or extracted from experiments.[3,4]

Alternatively, and despite its long recognized deficiencies, the semi-empirical extended Hückel theory (EHT) is still often employed in electronic calculations for periodic and nonperiodic systems,[5–9] mainly due to its simplicity and the chemical insight it provides.[10] In most EHT studies the associated Hückel parameters are transferred between different chemical environments with the only and rather ambiguous requirement of providing a *reasonable* description of the electronic structure of the system. In the transfer process, it is also quite common to vary the AOs' on-site energies self-consistently until a preselected charge distribution for the different atoms in the unit cell is achieved,[6,8,9] although the amount of charge transfer between the atoms, or even the assumption of atomic charge neutrality are somewhat dubious concepts and will in general lead to different electronic structures depending on the AO basis set selected.

Thus, the EHT has generally been regarded as a scheme capable of providing, at most, qualitative trends on the bonding chemistry and bonding geometry of the system.[5] Muller *et al.*[8] attempted a parametrization for nickel and aluminum via a fit to accurate band structures, and concluded that the EHT could not accurately reproduce **k**-resolved quantities such as the density of states $\rho(\vec{k})$ or the band structure, although Brillouin Zone integrated (or energy integrated) quantities presented a much better agreement with the accurate calculations. On the other hand, Nishida[7] achieved a remarkable fit for Si within the EHT formalism by defining a rather large parameter basis set that resembled a typical SK-TB parametrization. However, it is surprising that, to our knowledge, a systematic quantitative study on the accuracy attainable with the EHT when applied to different bulk materials has not yet been attempted.

In this contribution, we apply a new EHT parametrization scheme to different elemental and compound solids, which is based on the SK approach. Contrary to the general belief, we find that the EHT, when compared to the traditional SK tight-binding results,[3,4] can provide a similar level of accuracy while presenting several important advantages inherent to the theory itself, namely: (i) a considerable reduction in the number of parameters to be fitted, (ii) *natural* scaling laws for the AO's interactions and, (iii) an enhancement of the transferability of the parameters for their use in different chemical environments. Our approach is in essence similar to the recent TB parametrization of M.J. Mehl *et al.*,[11] who have generalized the extensively used set of TBP's of Ref. 3 (hereafter referred as DAP), in order not only to account for the dependence of the overlap and Hamiltonian matrix elements on distance, but also to reproduce total energy trends and elastic constants. To this end, they fit the TBP's of each element to accurate band-structure calculations for different structural phases at different lattice constants, whereas the on-site energies are made dependent on a *pseudoatomic* density specific for each elemental phase.[11] However, the fits involve up to around 70 parameters per element.

We explain our parametrization method in the next section, also providing tables with the optimized AO basis sets and the on-site energies for all the cases studied. In Sec. III, an outlook of our approach is given together with the conclusions of this work.

II. EHT PARAMETRIZATION SCHEME

Within the EHT (Ref. 10) an orthonormal AO basis set $\{\alpha i\}$ is chosen for each inequivalent atom i. Generally, the basis involves rather extended radial wave functions, although any other type of basis set may be employed as well. The Hamiltonian matrix elements $H_{\alpha i,\beta j}$ between any two AO's, α and β, centered at atoms i and $j(i \neq j)$, respectively, are approximated by setting them proportional to the corresponding overlap $O_{\alpha i,\beta j}$ according to $H_{\alpha i,\beta j} = K_{\alpha i,\beta j} \cdot O_{\alpha i,\beta j}$, where $K_{\alpha i,\beta j}$ only depends on the on-site energies of both elements, $E_{\alpha i}$ and $E_{\beta j}$. Despite the existence of different formula for $K_{\alpha i,\beta j}$,[6,12] we have employed in this work the form: $K_{\alpha i,\beta j} = K_{EHT} \times (E_{\alpha i} + E_{\beta j})/2$, where K_{EHT} is a dimensionless constant tradionally set to a value of 1.75.[13] It is important to notice from the above formula that the strength of the Hamiltonian matrix elements is weighted by the mean value of the on-site energies, so that a shift in

energy of these on-site parameters does not translate into a rigid shift in energy of the EHT-derived band structure. Therefore, and in order to avoid any arbitrariness in the origin of the energy scales, we have fixed the Fermi level for transition metals to -10 eV and the top of the valence band for semiconductors to -13 eV. We have then found that increasing K_{EHT} to 2.3 consistently provided better fits for all elements, although we recall that similar good fits may be obtained with $K_{EHT}=1.75$ if the Fermi level is lowered to around -20 eV.

Our EHT parametrization scheme is then as follows. We employ a minimal *spd* basis set per element, while each AO is described by a double-ζ Slater wave function. Apart from the on-site energies (E_s, E_p, and E_d), this leads to three parameters per l quantum number: the exponents ζ_1 and ζ_2 (with $\zeta_1<\zeta_2$), and the coefficient for the former, c_1. The second coefficient, c_2, is determined by imposing normalization of the wave function. For transition metals the optimization of the three AO parameters was found to be redundant for the *s* and *p* orbitals, and equally good fits could be obtained by fixing ζ_2 to a rather large value: $\zeta_2>20.0$. Since such a highly localized term gives a negligable contribution to the overlaps with neighboring orbitals, we explicitly omit it, while allowing the coefficient c_1 to take values smaller than 1.0 (i.e., the ζ_2 Slater orbital only contributes to the normalization of the wave function). For the *d* orbitals, on the contrary, we have found necessary to include the ζ_2 contribution. Hence, our transition metal fits comprise 10 parameters per elemental phase. In order to improve the transferability of the EHT-TBP's, we have also optimized the AO basis set of a given element simultaneously for different structural phases (e.g., Ti-fcc, -bcc, and -hcp), while the on-site energies have been treated as independent parameters for each phase. For the spin polarized phases of Fe, Co, and Ni, we have additionally varied the c_1 coefficient of the *d* orbitals independently for each spin, since the *d* bandwidths are larger for the spin minority bands than for the majority ones.

The accurate band structures used in the optimization of the EHT parameters for transition metals were calculated employing the DAP's two-center non-orthogonal set of TBP's. For the fits, we selected $N_k\approx 30-40$ representative **k** points both at high symmetry directions and at equispaced grid points inside the irreducible Brillouin Zone, and included all bands up to 4–5 eV above the Fermi level,[14] which was always fixed to -10 eV ($K_{EHT}=2.30$). We set a cut-off radius for the AO overlaps and interactions of $r_c=9.0$ Å for all cases, and checked that this value already provided well-converged energy bands.

The parameter optimization was carried out via conjugate gradient minimizations[15] of the root mean square deviation (rms) between the EHT bands and the accurate ones. In order to avoid the algorithm to home at undesired local minima we also seldom employed the simulated annealing optimization technique,[15] which does not require a good initial set of parameter values for locating the global minimum.

The final optimized AO basis sets are listed in Table I, while the on-site energies for each fitted elemental phase are given in Table II, together with some details of the fit. We also present in Fig. 1 energy bands, together with their respective accurate ones, for some representative phases. The accuracy of these EHT-derived parameters is mirrored by *rom* values below 100 meV for most cases. These values compare well with the accuracy of the fits obtained within the two- or three-center orthogonal approximation by DAP, although our EHT fits involve less than half the number of parameters for each phase. The transferability of the AO basis sets is evidenced by noting from Table II the good agreement obtained for the different phases considered for the elements Sc, Ti, Mn, Fe, Co, Ni, Zr, Tc, or Ru. Furthermore, an important point which renders our EHT-TBP's physically meaningful is the fact that they follow the expected trend of a stronger AO localization (i.e., larger χ_1 or c_1) as the corresponding on-site energy becomes lower in energy (i.e., the AO becomes more tightly bound). It is also worth mentioning that the fits obtained following the same scheme but employing a smaller cut-off radius ($r_c=5$ Å) are only slightly worse by roughly 40% than those given in Table II, even though the energy bands are not fully converged and the transferability of the TBP's is considerably worsened for such a small range of interactions.

A second test for the transferability of the AO basis sets consists in modifying the chemical environment in addition to the geometrical environment. To this end, we have also considered several compound materials: AlP, AlAs, GaP, and GaAs. We have performed the same type of optimization as described above, fitting the band structures of the four semiconductors together with those for Ga-fcc and Al-fcc simultaneously. For the latter, we have again used as the accurate bands those of DAP, while for the III-V compounds we employed the quasiparticle band structure calculations of X. Zhu *et al.*,[16] fixing the top of the valence band to -13 eV and including just the Γ, *X*, and *L* **k** points in the fit up to -5 eV. For the description of Ga we supressed the 3-*d* AO's since they are highly localized (yielding a very narrow *d* band in the metallic phase), and used the 4-*d* excited orbitals in order to improve the fit of the high-energy bands. Therefore, this calculation comprised four elements in six different phases, involving up to 62 parameters in total.

The resulting optimized EHT-TBP's are included in Tables I and II, following the same format as the one used above for the transition metals. This time, we find that, for the 6 elements involved, the *p* AO's need to be explicitly described by double-ζ Slater orbitals, while the *d* orbitals may be simplified to single-ζ (with c_1 as an additional parameter) for Ga and P. The corresponding band structures are displayed in Fig. 2, where the data points used for the semiconductor fits are indicated by open circles. We again confirm the good performance of the EHT-TBP's; for the semiconductors, although the number of data points fitted is just 14, the rms values obtained are remarkably small, implying that the energy gaps are accurately reproduced, whereas for the Ga and Al metallic phases we still find a satisfactory agreement. We also present in Fig. 2 (dotted lines) the bands deduced from the recently published set of orthogonal SK-TBP's of Jancu *et al.*,[4] which was restricted to the first nearest neighbors interactions. Despite the fact that Jancu *et al.* employed a larger basis set than ours, we consistently find a better fit to the pseudopotential results with our approach.

The transferability of the so derived As and P AO basis sets has next been tested by performing a further optimization for InAs, InP, and metallic In-fcc. During the simultaneous fit for the three phases, we kept fixed the AO param-

TABLE I. Optimized EHT AO basis sets after the parametrization procedure described in the text. Although all AO's are of the double-ζ Slater type, the ζ_2, and c_2 values are not included in the table whenever $\zeta_2 > 20.0$ (see text for further explanations).

	AO	ζ_1	c_1	ζ_2	c_2		AO	ζ_1	c_1	ζ_2	c_2
Sc	4*s*	1.325	0.575			Ti	4*s*	1.337	0.707		
	4*p*	1.111	0.624				4*p*	1.135	0.617		
	3*d*	1.332	0.527	4.172	0.690		3*d*	1.464	0.532	4.760	0.695
Cr	4*s*	1.426	0.753			Mn	4*s*	1.468	0.725		
	4*p*	1.210	0.632				4*p*	1.233	0.625		
	3*d*	1.676	0.502	4.688	0.683		3*d*	1.683	0.447	4.534	0.720
Fe	4*s*	1.594	0.777			Co	4*s*	1.561	0.665		
	4*p*	1.315	0.658				4*p*	1.282	0.616		
	3*d*	1.755	0.442	4.845	0.730		3*d*	1.724	0.393	4.765	0.769
Ni	4*s*	1.616	0.691			Cu	4*s*	1.705	0.614		
	4*p*	1.307	0.630				4*p*	1.340	0.648		
	3*d*	1.775	0.392	5.238	0.785		3*d*	1.855	0.367	6.770	0.842
Zr	5*s*	1.539	0.706			Nb	5*s*	1.615	0.772		
	5*p*	1.263	0.530				5*p*	1.285	0.602		
	4*d*	1.646	0.593	4.478	0.629		4*d*	1.761	0.587	4.335	0.603
Mo	5*s*	1.662	0.789			Tc	5*s*	1.647	0.803		
	5*p*	1.334	0.638				5*p*	1.365	0.623		
	4*d*	1.900	0.573	4.693	0.618		4*d*	1.962	0.546	4.870	0.645
Ru	5*s*	1.729	0.769			Rh	5*s*	1.697	0.786		
	5*p*	1.408	0.667				5*p*	1.415	0.638		
	4*d*	2.048	0.538	5.500	0.676		4*d*	2.042	0.457	4.857	0.711
Pd	5*s*	1.816	0.741			Ag	5*s*	1.846	0.589		
	5*p*	1.452	0.695				5*p*	1.475	0.610		
	4*d*	2.120	0.496	6.622	0.753		4*d*	2.076	0.325	4.907	0.812
Cd	5*s*	1.703	0.570			W	6*s*	2.216	0.673		
	5*p*	1.281	0.508				6*p*	1.642	0.603		
	5*d*	1.237	0.453				5*d*	2.132	0.546	5.139	0.665
Re	6*s*	2.253	0.723			Ir	6*s*	2.252	0.651		
	6*p*	1.615	0.703				6*p*	1.712	0.631		
	5*d*	2.194	0.517	4.926	0.667		5*d*	2.287	0.432	4.929	0.727
Pt	6*s*	2.294	0.625			Au	6*s*	2.309	0.600		
	6*p*	1.715	0.681				6*p*	1.740	0.622		
	5*d*	2.318	0.429	5.327	0.749		5*d*	2.291	0.349	5.065	0.799
Ga	4*s*	2.041	0.662			Al	3*s*	1.657	0.749		
	4*p*	1.616	0.705	5.835	0.596		3*p*	1.312	0.750	4.679	0.492
	4*d*	1.028	0.636				3*d*	0.860	0.609	4.245	0.717
In	5*s*	2.110	0.580								
	5*p*	1.770	0.670								
	5*d*	1.089	0.527								
C[a]	2*s*	2.125	0.790			Si	3*s*	1.864	0.720		
	2*p*	1.269	0.177	2.271	0.851		3*p*	1.470	0.303	1.813	0.705
	3*d*	0.906	0.687				3*d*	0.675	0.671	1.705	0.485
P	3*s*	2.131	0.769			As	4*s*	2.344	0.634		
	3*p*	1.859	0.633	2.479	0.384		4*p*	2.102	0.753	7.588	0.539
	3*d*	0.797	0.709				4*d*	0.918	0.660	3.926	0.681

[a] $K_{EHT} = 2.8$ (see text).

eters of As and P to the values given in Table I, while their on-site energies were varied independently for each phase, together with the parameters relevant to In. The number of parameters involved in the fit was then 22. Accurate bands were extracted from Ref. 16 and from DAP. The results are again encouraging, as we obtain rms values of just 32 and 42 meV for the two semiconductor phases and 111 meV for In-fcc (see Tables I and II), reflecting the high transferability of the AO basis sets. We also show in Fig. 2 the corresponding band structure plots.

For completeness, we have finally derived EHT parameters for Si, diamond and SiC, for which we placed the top of

TABLE II. Optimized on-site energies, in eV, for the different bulk phases considered in this work, together with the rms value and the maximum energy deviation of any of the fitted bands, Δ_{max}, corresponding to the final fit between the accurate band structures and the EHT derived ones. The element-specific AO basis employed for each phase (third column) are given in Table I. All rms and Δ_{max} values are in meV, while the lattice parameter for each phase, a, is in Å. Notice that for the spin-polarized phases of Fe, Co, and Ni, ↑(↓) refers to the spin majority (minority) bands, while the c_1 coefficients for the d orbitals have also been optimized independently, attaining values different from those given in Table I (see footnote).

Phase	a	Element	E_s	E_p	E_d	rms	Δ_{max}
Sc-hcp	3.31	Sc	−8.419	−5.989	−8.391	51	215
Sc-bcc	3.54	Sc	−8.305	−5.917	−8.453	41	139
Ti-hcp	2.95	Ti	−8.131	−6.124	−9.308	64	259
Ti-fcc	4.10	Ti	−7.957	−5.986	−9.145	52	148
Ti-bcc	3.31	Ti	−7.879	−5.950	−8.943	36	124
Cr-bcc	2.88	Cr	−8.492	−6.269	−10.635	44	118
Mn-bcc	2.86	Mn	−8.906	−6.630	−11.162	35	96
Mn-fcc	3.60	Mn	−8.700	−6.283	−10.823	37	167
Fe-bcc	2.80	Fe	−8.994	−6.177	−11.323	34	92
Fe-bcc ↑	2.86	Fe[a]	−9.136	−6.319	−11.855	38	197
Fe-bcc ↓	2.86	Fe[b]	−9.275	−6.582	−10.273	74	216
Co-fcc	3.46	Co	−9.543	−6.685	−11.689	51	433
Co-hcp	2.51	Co	−9.683	−6.894	−11.699	36	113
Co-hcp ↑	2.51	Co[c]	−9.783	−7.226	−12.600	54	342
Co-hcp ↓	2.51	Co[d]	−9.673	−6.890	−10.910	64	368
Ni-fcc	3.46	Ni	−9.523	−6.553	−11.744	32	127
Ni-fcc ↑	3.52	Ni[e]	−9.867	−6.962	−12.210	36	199
Ni-fcc ↓	3.52	Ni[f]	−9.758	−6.779	−11.526	32	143
Cu-fcc	3.61	Cu	−10.563	−6.780	−12.869	36	268
Zr-hcp	3.23	Zr	−8.017	−6.033	−9.022	81	267
Zr-fcc	4.40	Zr	−7.886	−5.766	−8.920	103	487
Zr-bcc	3.49	Zr	−7.691	−5.600	−8.722	108	335
Nb-bcc	3.30	Nb	−7.768	−5.246	−9.318	112	305
Mo-bcc	3.15	Mo	−8.365	−5.666	−10.855	97	273
Tc-hcp	2.74	Tc	−8.406	−5.804	−11.386	115	308
Tc-fcc	3.84	Tc	−8.142	−5.674	−11.324	83	258
Ru-hcp	2.70	Ru	−8.953	−5.778	−12.352	120	368
Ru-fcc	3.81	Ru	−8.450	−5.598	−11.871	60	168
Rh-fcc	3.80	Rh	−8.412	−5.854	−12.388	29	104
Pd-fcc	3.89	Pd	−8.781	−5.627	−12.346	32	130
Ag-fcc	4.06	Ag	−9.925	−6.437	−14.705	23	117
Cd-fcc	4.34	Cd	−10.743	−7.779	−6.441	64	179
W-bcc	3.16	W	−11.013	−6.062	−10.806	110	322
Re-hcp	2.76	Re	−10.959	−5.944	−11.337	79	311
Ir-fcc	3.84	Ir	−11.548	−6.650	−13.089	51	272
Pt-fcc	3.92	Pt	−11.851	−6.304	−13.058	46	176
Au-fcc	4.08	Au	−12.131	−6.760	−14.000	39	185
Diamond	3.57	C	−22.649	−14.871	−3.440	122	245
Si	5.43	Si	−18.137	−11.277	−5.336	103	160
SiC	4.36	C	−19.545	−12.821	−1.705	77	190
		Si	−19.525	−11.858	−6.415		
Al-fcc	4.02	Al	−13.133	−8.525	−5.141	114	477
Ga-fcc	4.14	Ga	−14.660	−8.400	−3.429	140	452
In-fcc	4.73	In	−13.907	−8.294	−3.864	111	401
AlP	5.46	Al	−15.645	−10.211	−5.144	12	29
		P	−20.236	−12.437	−3.845		
AlAs	5.66	Al	−15.720	−10.464	−5.278	12	24
		As	−21.439	−12.531	−4.107		
GaP	5.45	Ga	−17.544	−10.607	−3.544	26	83
		P	−20.615	−12.714	−5.196		

TABLE II. (*Continued*).

Phase	a	Element	E_s	E_p	E_d	rms	Δ_{max}
GaAs	5.65	Ga	−17.629	−10.766	−3.507	12	31
		As	−21.764	−12.822	−5.488		
InP	5.87	In	−16.845	−10.070	−1.354	42	80
		P	−20.617	−12.981	−5.696		
InAs	6.04	In	−17.078	−10.794	−4.279	32	72
		As	−21.530	−12.776	−4.831		

[a] $c_1 = 0.412$.
[b] $c_1 = 0.508$.
[c] $c_1 = 0.360$.
[d] $c_1 = 0.437$.
[e] $c_1 = 0.376$.
[f] $c_1 = 0.403$.

the valence band at −13, −15, and −14 eV, respectively (we again set $r_c = 9$ Å). Accurate band structures for the three phases were taken from the quasiparticle calculations of M. Rholfing *et al.*[17] For diamond and Si we also included in the fit their respective conduction-band minima (CBM) since they are not located at high-symmetry points but along the $\Gamma-(\Delta)-X$ line. Moreover, and in order to improve the fit around the gap region, we included an energy dependent weight function in the rms evaluation so that data points close in energy to the gap were given special emphasis. On the other hand, owing to the large dispersion of the diamond bands, we found that accurate results throughout the entire energy range could only be obtained if K_{EHT} was considerably increased. Hence, in the EHT optimization, we kept $K_{EHT} = 2.3$ for Si, but used $K_{EHT} = 2.8$ for diamond. In the SiC case, we retained these values for the Si-Si and C-C interactions, respectively, while for the Si-C interactions we employed their mean value $K_{EHT} = 2.55$. From the results listed in the tables and shown in Fig. 2, we still find a satisfactory performance of the EHT, although the rms values are

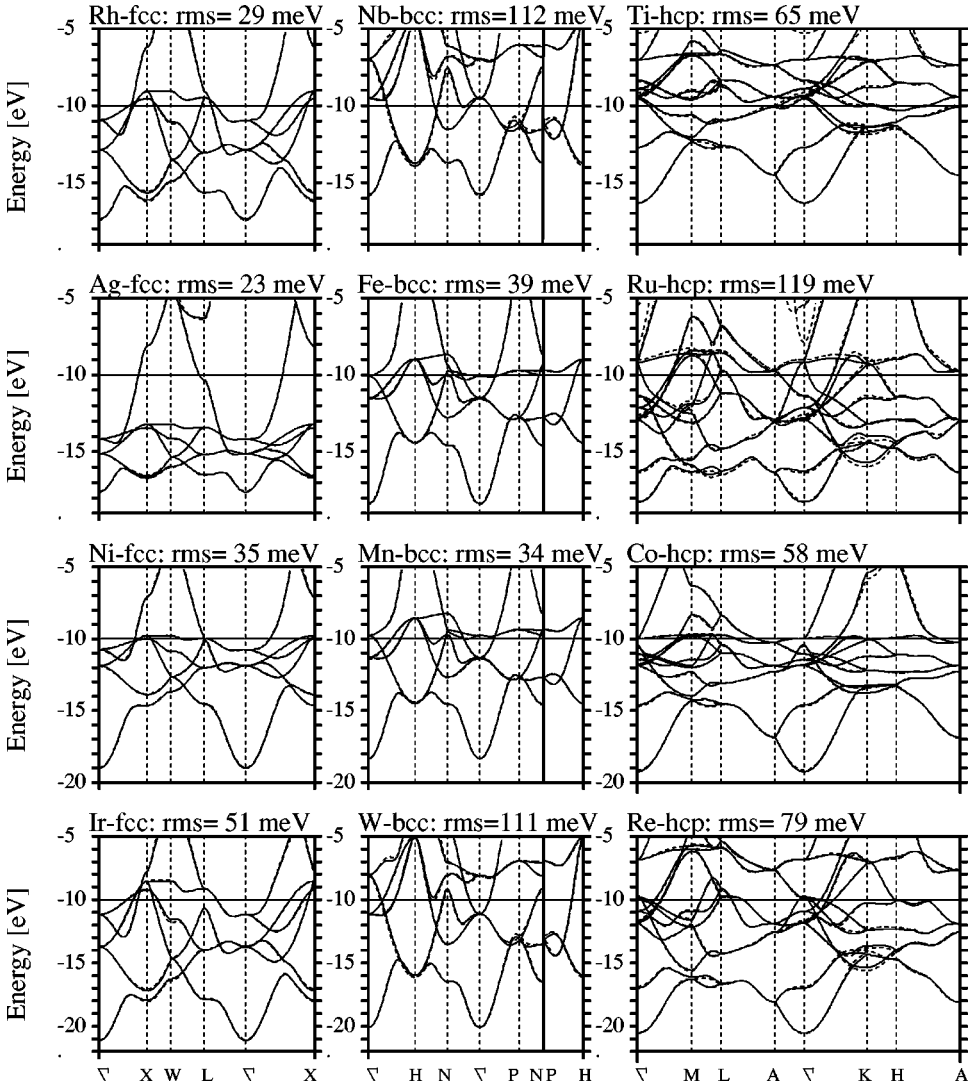

FIG. 1. Best fit EHT band structures (solid lines) and those obtained with the two-center nonorthogonal TBP set of Ref. 3 (dotted lines) for some selected bulk transition metals. The accurate band structures have been rigidly shifted in energy so that the Fermi level lies at −10 eV (horizontal solid lines). On top of each graph, the fitted elemental phase and its corresponding rms value is indicated.

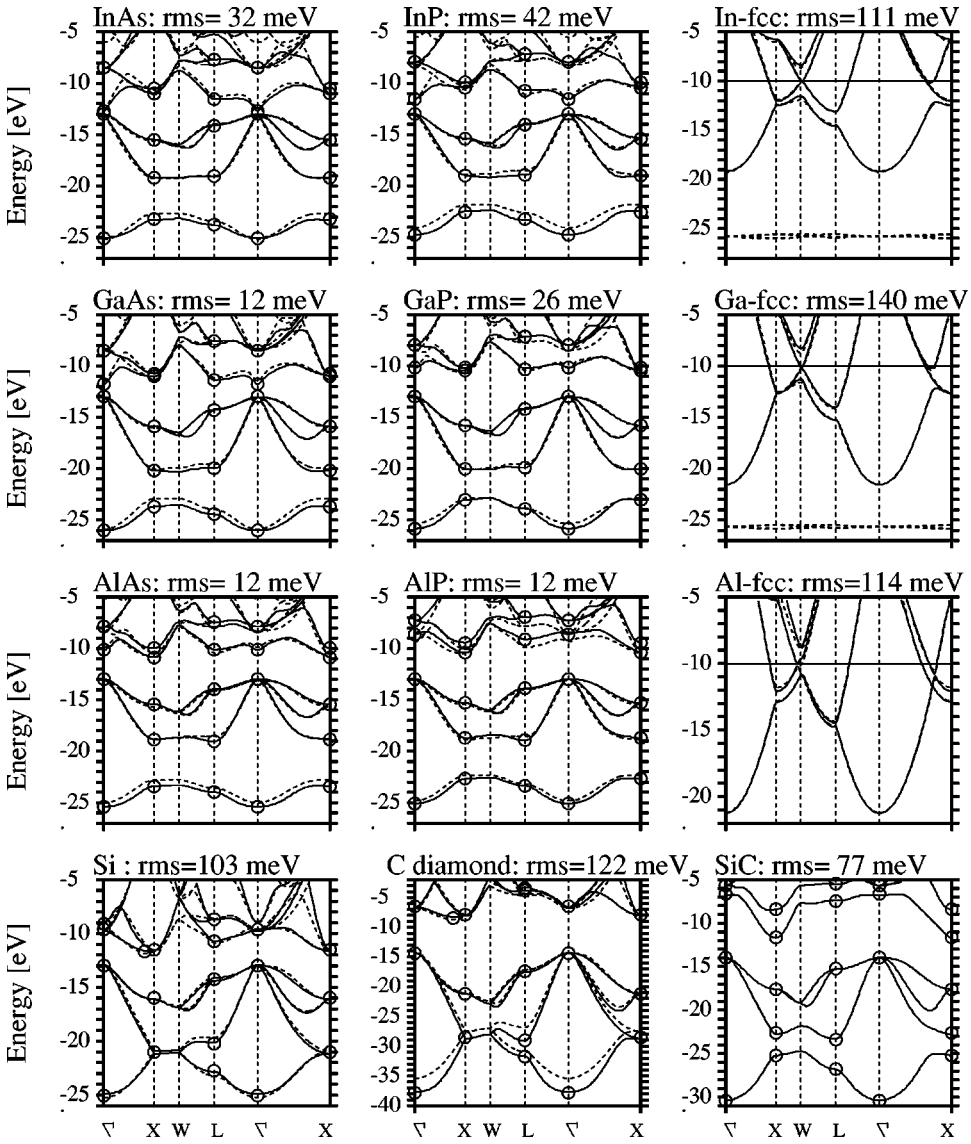

FIG. 2. Best fit EHT band structures for the bulk phases indicated on top of each graph (solid lines). For all semiconductors, diamond and SiC, the accurate band structures of Refs. 16 and 17 are indicated by small open circles. They have been shifted in energy so that the top of the valence band is located at -13 eV except for diamond (-15 eV) and SiC (-14 eV). The dotted lines correspond to band structures obtained with the two-center orthogonal TBP set of Ref. 4, again shifted in energy by the same amounts. Graphs for Al, Ga and In are the same as Fig. 1.

somewhat larger than those obtained for the III-V semiconductors, attaining values close to 100 meV. The EHT (accurate) energy gaps are 5.85 eV (5.67 eV) for C and 1.30 eV (1.31 eV) for Si, while the CBM are correctly located within the $\Gamma - X$ line. We should notice, however, that the energy difference between the CBM and the first conduction band at X_{1c} is around half the value obtained in Ref. 17 both for Si and diamond. Nevertheless, we checked that this discrepancy could be removed by further increasing the rms weights around the gap region, although this lead to a poorer description of the lowest valence bands.

III. FINAL DISCUSSION AND CONCLUSIONS

We have presented a EHT parametrization scheme for bulk materials, which employs a very reduced parameter basis set and still provides transferable AO basis while maintaining an accurate description of the electronic structure.[18] The main difference from the traditional TB schemes is the explicit definition of the AO's, which might look at first glance as a disadvantage, since it requires the calculation of the overlap matrix elements. However, the computational effort involved in constructing the actual overlap $O(\mathbf{k})$ and Hamiltonian $H(\mathbf{k})$ matrices is minimal (only two-center integrals plus the simple EHT formula are involved) and more importantly, for a fixed cut-off radius r_c, it scales linearly with the number of orbitals in the unit cell. Moreover, we regard the explicit use of AO's as advantageous, particularly in what concerns the transferability of the EHT-TBP's, since the dependence of the overlap terms $O_{\alpha i,\beta j}$ on the interatomic distance d_{ij} readily provides a natural scaling law that is not restricted to small variations of d_{ij}. A further advantage is the possibility to obtain the local density of states $\rho(E,\vec{r})$, while the traditional TB methods only provide real space integrated quantities.

We should finally stress that the TBP's deduced in this work do not correspond to the best fits attainable with a Hückel type Hamiltonian. There still exists a great freedom for increasing the actual parameter basis set, such as the use of triple- or multi-ζ Slater orbitals or any other type of AO's, the inclusion of three-center corrections[2,3,19] or using K_{EHT} as a further parameter for each pair of orbital interactions. Indeed, the latter option seems necessary in the case of diamond in order to attain an accurate fit for the lowest energy bands. Furthermore, if one is only interested in the electronic

structure within a small energy window (such is the case for transport properties in metals or optical properties in semiconductors), the accuracy may also be improved by using larger weights in the calculation of the rms for the data points contained in the energy range of interest. We also believe that the present scheme may be easily modified in order to reproduce total energy trends,[11] although such a generalization is beyond the scope of this work. On the other hand, one may impose further restrictions on the basis set depending on the specific problem to be tackled without deteriorating too much the fit (e.g., specific AO decay lengths at surfaces, small cut-off radius for huge unit cells, etc.).

In conclusion, we hope that the present EHT parametrization scheme will be fruitful for future tight-binding studies.

ACKNOWLEDGMENTS

J.C. acknowledges financial support from the Spanish Ministerio de Educación y Ciencia and from the Spanish CICYT under Contract No. PB96-0916.

*Author to whom correspondence should be addressed. Electronic address: Jcerda@icmm.csic.es

[1] P. Ordejon, E. Artacho, and J.M. Soler, Phys. Rev. B **53**, 10 441 (1996).

[2] J.C. Slater and G.F. Koster, Phys. Rev. **94**, 1498 (1954).

[3] D.A. Papaconstantopoulos, *Handbook of the Band Structure of Elemental Solids* (Plenum, New York, 1986).

[4] J.-M. Jancu, R. Scholz, F. Beltram, and F. Bassani, Phys. Rev. B **57**, 6493 (1998).

[5] T.R. Ward, R. Hoffmann, and M. Shelef, Surf. Sci. **289**, 85 (1993); D.Lj. Vucković, S.A. Jansen, and R. Hoffmann, Langmuir **6**, 732 (1990); M.C. Zonnevylle and R. Hoffmann, *ibid.* **3**, 452 (1987).

[6] Z. Yang, K. Zhang, and X. Xie, Surf. Sci. **382**, 100 (1997); H. Fu, L. Ye, K. Zhang, and X. Xie, *ibid.* **341**, 273 (1995); I. Efremenko and M. Sheintuch, *ibid.* **414**, 148 (1998); P. Sonnet, L. Stauffer, S. Saintenoy, C. Piffi, P. Wetzel, G. Gewinner, and C. Minot, Phys. Rev. B **56**, 15 171 (1997); C. Noce and M. Cuoco, *ibid.* **59**, 2659 (1999).

[7] M. Nishida, Phys. Rev. B **58**, 7103 (1998).

[8] D.A. Muller, P.E. Batson, and J. Silcox, Phys. Rev. B **58**, 11 970 (1998).

[9] J. Cerdá, A. Yoon, M.A. Van Hove, P. Sautet, M. Salmerón, and G.A. Somorjai, Phys. Rev. B **56**, 15 900 (1997); J. Cerdá, M.A. Van Hove, P. Sautet, and M. Salmerón, Surf. Sci. **409**, 145 (1998); M.-L. Bocquet, J. Cerdá, and P. Sautet, Phys. Rev. B **59**, 15 437 (1999).

[10] R. Hoffmann, Rev. Mod. Phys. **60**, 601 (1988).

[11] M.J. Mehl and D.A. Papaconstantopoulos, Phys. Rev. B **54**, 4519 (1996).

[12] J.H. Ammeter, H.-B. Bürgi, J.C. Thibeault, and R. Hoffmann, J. Am. Chem. Soc. **100**, 3686 (1978).

[13] The use of the corrected formula proposed in Ref. 12, although it removes any negative Mulliken populations, consistently leads to worse fits due to an unphysical increase of the interactions between AO's very distant in energy.

[14] We seldom skipped from the fit high-energy bands whenever they had not been accurately fitted in Ref. 3 (e.g., the 13th and 14th bands at Γ for Ru-hcp).

[15] W. H. Press, B.P. Flannery, S.A. Teukolsky, and W.T. Vetterling, *Numerical Recipes: The Art of Scientific Computing* (Cambridge University Press, Cambridge, 1989).

[16] X. Zhu and S.G. Louie, Phys. Rev. B **43**, 14 142 (1991).

[17] M. Rholfing, P. Krüger, and J. Pollmann, Phys. Rev. B **48**, 17 791 (1993).

[18] Please contact the authors for more information on the fitting procedure and the final EHT parameters. The EHT-TB program may be supplied upon request.

[19] M.D. Stiles, Phys. Rev. B **55**, 4168 (1997).